

**$\beta$  decay of  $^{36}\text{Mg}$  and  $^{36}\text{Al}$ : Identification of a  $\beta$ -decaying isomer in  $^{36}\text{Al}$** 

R. S. Lubna<sup>1,\*</sup>, S. N. Liddick,<sup>1,2</sup> T. H. Ogunbuku,<sup>1,3</sup> A. Chester,<sup>1</sup> J. M. Allmond,<sup>4</sup> Soumik Bhattacharya,<sup>5</sup> C. M. Campbell,<sup>6</sup> M. P. Carpenter,<sup>7</sup> K. L. Childers,<sup>8,2</sup> P. Chowdhury,<sup>9</sup> J. Christie,<sup>10</sup> B. R. Clark,<sup>3</sup> R. M. Clark,<sup>6</sup> I. Cox,<sup>10</sup> H. L. Crawford,<sup>6</sup> B. P. Crider,<sup>3</sup> A. A. Doetsch,<sup>1,11</sup> P. Fallon,<sup>6</sup> A. Frotscher,<sup>6</sup> T. Gaballah,<sup>3</sup> T. J. Gray,<sup>4</sup> R. Grzywacz,<sup>7</sup> J. T. Harke,<sup>12</sup> A. C. Hartley,<sup>1,2</sup> R. Jain,<sup>1,11</sup> T. T. King,<sup>4</sup> N. Kitamura,<sup>10</sup> K. Kolos,<sup>12</sup> F. G. Kondev,<sup>7</sup> E. Lamere,<sup>9</sup> R. Lewis,<sup>8,2</sup> B. Longfellow,<sup>8,11,12</sup> S. Lyons,<sup>8,†</sup> S. Luitel,<sup>3</sup> M. Madurga,<sup>10</sup> R. Mahajan,<sup>1</sup> M. J. Mogannam,<sup>1,2</sup> C. Morse,<sup>13</sup> S. K. Neupane,<sup>10</sup> W.-J. Ong,<sup>12</sup> D. Perez-Loureiro,<sup>10</sup> C. Porzio,<sup>6</sup> C. J. Prokop,<sup>14</sup> A. L. Richard,<sup>8,‡</sup> E. K. Ronning,<sup>1,2</sup> E. Rubino,<sup>1,‡</sup> K. Rykaczewski,<sup>4</sup> D. Seweryniak,<sup>7</sup> K. Siegl,<sup>10</sup> U. Silwal,<sup>3</sup> M. Singh,<sup>10</sup> D. P. Siwakoti,<sup>3</sup> D. C. Smith,<sup>3</sup> M. K. Smith,<sup>8</sup> S. L. Tabor,<sup>5</sup> T. L. Tang,<sup>5</sup> Vandana Tripathi,<sup>5</sup> A. Volya,<sup>5</sup> T. Wheeler,<sup>1,11</sup> Y. Xiao,<sup>3</sup> and Z. Xu<sup>10</sup>

<sup>1</sup>Facility for Rare Isotope Beams, Michigan State University, East Lansing, Michigan 48824, USA

<sup>2</sup>Department of Chemistry, Michigan State University, East Lansing, Michigan 48824, USA

<sup>3</sup>Department of Physics and Astronomy, Mississippi State University, Mississippi State, Mississippi 39762, USA

<sup>4</sup>Physics Division, Oak Ridge National Laboratory, Oak Ridge, Tennessee 37831, USA

<sup>5</sup>Department of Physics, Florida State University, Tallahassee, Florida 32306, USA

<sup>6</sup>Nuclear Science Division, Lawrence Berkeley National Laboratory, Berkeley, California 94720, USA

<sup>7</sup>Argonne National Laboratory, Argonne, Illinois 60439, USA

<sup>8</sup>National Superconducting Cyclotron Laboratory, Michigan State University, East Lansing, Michigan 48824, USA

<sup>9</sup>Department of Physics, University of Massachusetts Lowell, Lowell, Massachusetts 01854, USA

<sup>10</sup>Department of Physics and Astronomy, University of Tennessee, Knoxville, Tennessee 37966, USA

<sup>11</sup>Department of Physics and Astronomy, Michigan State University, East Lansing, Michigan 48824, USA

<sup>12</sup>Lawrence Livermore National Laboratory, Livermore, California 94550, USA

<sup>13</sup>Brookhaven National Laboratory, Upton, New York 11973, USA

<sup>14</sup>Los Alamos National Laboratory, Los Alamos, New Mexico 87545, USA



(Received 29 March 2023; accepted 21 July 2023; published 31 July 2023)

The level structure of  $^{36}\text{Al}$  has been studied via  $\beta$  decay of  $^{36}\text{Mg}$  at the Facility for Rare Isotope Beams (FRIB) and the National Superconducting Cyclotron Laboratory (NSCL). A long-lived isomer in  $^{36}\text{Al}$  was identified which decays by  $\beta$  to an excited state of  $^{36}\text{Si}$ . The ground state and the isomeric state of  $^{36}\text{Al}$  were found to populate different energy levels of  $^{36}\text{Si}$ . The results from the two data sets in the present work complement each other. Configuration interaction calculations performed with the FSU shell-model Hamiltonians provide reasonable descriptions to the experimental observations and offer insight into future improvements of the theoretical interpretation.

DOI: [10.1103/PhysRevC.108.014329](https://doi.org/10.1103/PhysRevC.108.014329)

## I. INTRODUCTION

The evolution of shell structure from stable to exotic nuclei is one of the primary interests of nuclear structure research as it plays a fundamental role in our understanding of nuclear interactions. Systematic study of the nuclei along isotopic and isotonic chains can provide insight into the relative positions of the salient single-particle orbitals as a progression is made from stable to exotic nuclei. It is also possible that dramatic changes are encountered, such as the rapid development of collectivity [1–4]. The Al isotopes are considered to be in a

transitional region [5–9] between the nuclei with ground states dominated by normal and intruder configurations around the  $N = 20$  island of inversion (IoI). Therefore, they play a crucial role in our understanding of the structural evolution. Despite their importance as a bridge between normal and intruder dominated configurations the neutron-rich Al isotopes are less explored as compared to the surrounding even- $Z$  nuclei.

In this article we report the first identification of a  $\beta$ -decaying isomeric state in  $^{36}\text{Al}$ . In two previous studies, the half-life of  $^{36}\text{Al}$  was reported as 90(40) ms [10] and about 14 ms [11] (value extracted from Fig. 1 of the reference) with a neutron-emission probability 55(11)%. No information on the level structure was available. We report the level structure populated via  $\beta$  decay of  $^{36}\text{Mg}$ . Further, we disentangle the energy levels of  $^{36}\text{Si}$  populated in either the  $\beta$ -decay chain  $^{36}\text{Mg} \rightarrow ^{36}\text{Al} \rightarrow ^{36}\text{Si}$  or from the decay of directly produced  $^{36}\text{Al}$ , which have provided clear evidence of the existence of a low-lying  $\beta$ -decaying isomeric state in  $^{36}\text{Al}$ .

\*lubna@frib.msu.edu

<sup>†</sup>Present address: Pacific Northwest National Laboratory, Richland, WA 99352, USA.

<sup>‡</sup>Present address: Lawrence Livermore National Laboratory, Livermore, California 94550, USA.

Theoretical calculations were performed using the configuration interaction derived from the FSU shell-model Hamiltonian [12,13] to interpret the structure of the mass  $A = 36$  isobars reported in this article. The calculations strongly support the presence of an isomer in  $^{36}\text{Al}$  and suggests future prospects for improving the existing theoretical models.

## II. EXPERIMENTAL DETAILS

The experiments to study the  $\beta$  decay of  $^{36}\text{Mg}$  and  $^{36}\text{Al}$  were conducted at the National Superconducting Cyclotron Laboratory (NSCL) and later at the Facility for Rare Isotope Beams (FRIB) at Michigan State University. In the first experiment at NSCL, a primary beam of  $^{48}\text{Ca}$  with 140 MeV/nucleon and 80 pnA intensity was impinged on a  $^9\text{Be}$  target of 642 mg/cm<sup>2</sup> thickness. The primary beam fragmented by the  $^9\text{Be}$  target was passed through the A1900 fragment separator [14] using a full 5% momentum acceptance. A wedge-shaped Al degrader of 120 mg/cm<sup>2</sup> thickness was employed at the dispersive image plane of the A1900. The radioactive cocktail beam centered around  $^{33}\text{Na}$  was then delivered to the experimental  $\beta$ -decay station. The beam was passed through two Si PIN detectors which provided the energy loss and time of flight relative to the scintillator at the intermediate dispersive image plane of the A1900 and the PIN detectors. This information was employed for the particle identification of the ions. The ions were then implanted in a CeBr<sub>3</sub> scintillator placed in the downstream side of the PIN detectors. The implantation detector was coupled with a position-sensitive photomultiplier tube (PSPMT) with one dynode and a  $16 \times 16$  pixelated anode grid with a total 256  $3 \text{ mm} \times 3 \text{ mm}$  anode pixels. The implantation detector was surrounded by 16 segmented germanium detectors (SeGa) [15] and 15 LaBr<sub>3</sub> detectors in order to record the  $\beta$ -delayed  $\gamma$ -ray transitions. Temporal and spatial correlations were performed between the ions and the decays.

In the second experiment at FRIB, a  $^{48}\text{Ca}$  primary beam was accelerated through the FRIB LINAC to an energy of 172.3 MeV/nucleon and was impinged on a 8.89 mm thick  $^9\text{Be}$  target. The fragmented beam was passed through the preseparator with a magnetic rigidity of  $B\rho = 5.100 \text{ Tm}$  and through the Advanced Rare Isotope Separator (ARIS) [16] which selected a cocktail beam centered around  $^{42}\text{Si}$  with a full momentum acceptance of 5%. The fragments were then delivered to the FRIB Decay Station Initiator (FDSi) [17,18]. A fast timing scintillator of 2 mm thickness followed by two Si PIN detectors, each 500  $\mu\text{m}$  thick, were used upstream of the implantation detector for the particle identification (PID). The energy lost by the ions in PIN2 was also plotted against the time of flight between the ARIS scintillator and the scintillator at the decay station in order to generate the PID as shown in Fig. 1 of Ref. [19]. At the center of the decay station, a 5 mm thick YSO scintillator implantation detector was placed [20]. The implantation detector was segmented into  $48 \times 48$  pixels with  $1 \text{ mm} \times 1 \text{ mm}$  dimensions. The YSO detector was flanked by two scintillator veto detectors immediately upstream and downstream, with the thickness of 2 mm and 5 mm, respectively. The implantation detector was surrounded by 11 HPGe clover detectors and 15 fast-timing

LaBr<sub>3</sub> detectors from one side and the neutron detector array VANDLE [21,22] from the other side.  $\beta$  decays were correlated with the ions based on temporal and spatial information, analogous to the treatment of the NSCL data.

In this work, the FRIB data are included to confirm and complement the results from the NSCL data. The FRIB data, though of lower statistics, provided cleaner  $\gamma$ -ray spectra which have added an extra confirmation to the observations from the NSCL experiment.

## III. ANALYSES AND RESULTS

The  $\beta$ -delayed  $\gamma$ -ray spectra following the  $^{36}\text{Mg} \rightarrow ^{36}\text{Al}$  decay in the two experiments are shown in Fig. 1. The ground-state transition at 1408 keV from the  $\beta$ -0n grand-daughter  $^{36}\text{Si}$  is present in the decay of  $^{36}\text{Mg}$  in both data sets, as seen in Fig. 1(a,b). Another peak at 1109 keV, which was reported in Ref. [23] and was suggested as belonging to one of  $^{34-36}\text{Si}$  is assigned to  $^{36}\text{Si}$  in the current analysis. The  $\gamma$ - $\gamma$  coincidence from the NSCL experiment confirms the 1109 keV peak belongs to  $^{36}\text{Si}$  as shown in Fig. 1(c). We place the 1109 keV peak on top of the 1408 keV level in the level scheme of  $^{36}\text{Si}$ . The presence of  $\beta$ -1n daughter  $^{35}\text{Al}$  and grand-daughter  $^{35}\text{Si}$  were confirmed in both the experiments as the known peaks correspond to the ground-state transitions 803 keV and 910 keV, respectively are clear in Fig. 1.

A peak at 657 keV was also observed in the  $\beta$ -delayed  $\gamma$ -ray spectrum of  $^{36}\text{Mg}$  in both the experiments as seen in Fig. 1. A transition at 657 keV was reported before in  $^{34}\text{Al}$ , populated via an intermediate-energy Coulomb excitation, with a tentative  $3^-$  spin-parity assignment [24]. A subsequent study of  $^{36}\text{Mg}$   $\beta$  decay also observed a 657 keV  $\gamma$  ray [23]

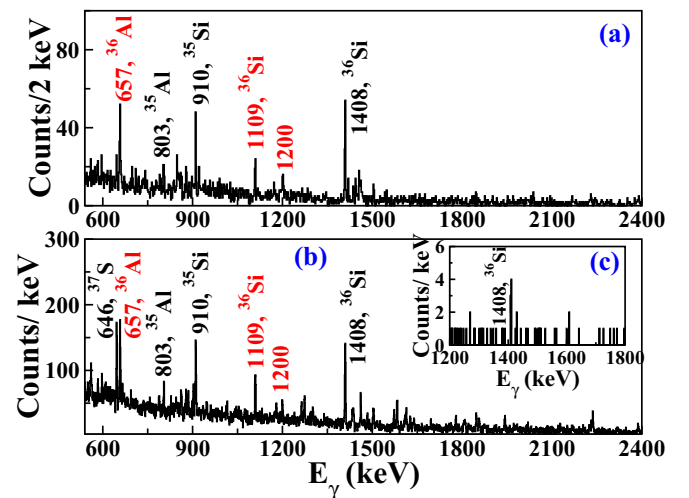


FIG. 1. (a) The  $\beta$ -delayed  $\gamma$ -ray spectrum observed in the FRIB experiment within the 100 ms time window following the arrival of an ion of  $^{36}\text{Mg}$ . (b) The  $\beta$ -delayed  $\gamma$ -ray spectrum of the same isotope within the 100 ms time window as observed in the NSCL experiment. (c) The spectrum in the inset shows the 1109 keV gate confirming the  $\gamma$ - $\gamma$  coincidence with the 1408 keV peak in the NSCL data. The peaks labeled in red are newly assigned (or observed) in the current analysis.

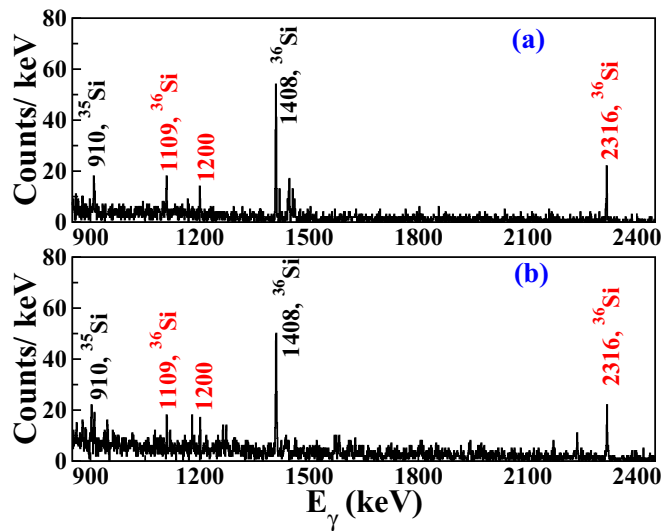


FIG. 2. (a)  $\beta$ -delayed  $\gamma$ -ray spectrum of  $^{36}\text{Al}$  decay achieved from the FRIB experiment. A 100 ms time window between the  $^{36}\text{Al}$  ions and the subsequent decays was considered. (b)  $\beta$ -delayed  $\gamma$ -ray spectrum of  $^{36}\text{Al}$  decay obtained from the NSCL experiment. A temporal correlation of 100 ms between the implants and the decay events was considered. The peaks labeled in red are newly assigned (or observed) in the current analysis.

and assumed it belonged to  $^{34}\text{Al}$  based on the similar energy to Ref. [24]. However, no other known  $\gamma$ -ray transitions from  $^{34}\text{Al}$  have been observed in Ref. [24] and the transition at

657 keV has not been observed in previous works studying  $^{34}\text{Al}$  [9,25]. Furthermore, if the 657 keV peak observed in the present work belongs to  $^{34}\text{Al}$ , the probability of two-neutron emission would need to be significantly larger than that of one neutron emission based on the intensities of the relevant transitions in  $\gamma$ -ray spectrum seen in Fig. 1. The neutron emission probability of  $^{36}\text{Mg}$  was measured and reported (preliminary result) in Ref. [11] as 48(12)%. Considering the arguments above, we assign the 657 keV transition to  $^{36}\text{Al}$ , though some possible contributions from  $^{34}\text{Al}$  can not be ruled out. We propose a state at 657 keV, decays by a  $\gamma$ -ray transition of the same energy, that is directly populated by the  $\beta$  decay of  $^{36}\text{Mg}$ . The most likely spin and parity for the new level established in  $^{36}\text{Al}$  is  $1^+$  considering it is populated quite strongly (a likely Gamow-Teller transition) from the  $0^+$  ground state of  $^{36}\text{Mg}$ . This assignment then constrains the spin-parity of the level to which this state will decay.

No other  $\gamma$ -ray transitions have been observed that could be assigned to  $^{36}\text{Al}$ . We do note that in Fig. 1. There is an additional transition visible at 1200 keV. We will return to this transition later.

The  $^{36}\text{Al} \rightarrow ^{36}\text{Si}$  decay was also studied following the direct production of  $^{36}\text{Al}$  in the fragmentation reactions. The  $\beta$ -delayed  $\gamma$ -ray spectra observed in the both experiments are shown in Fig. 2. The 1408 keV  $2^+ \rightarrow 0^+$  ground-state transition of  $^{36}\text{Si}$  is present in both spectra. The ground-state transition at 910 keV from the  $\beta$ -1n daughter  $^{35}\text{Si}$  is also clear in both measurements. A  $\gamma$ -ray transition at 2316 keV was observed which is assigned to  $^{36}\text{Si}$ , and placed feeding the

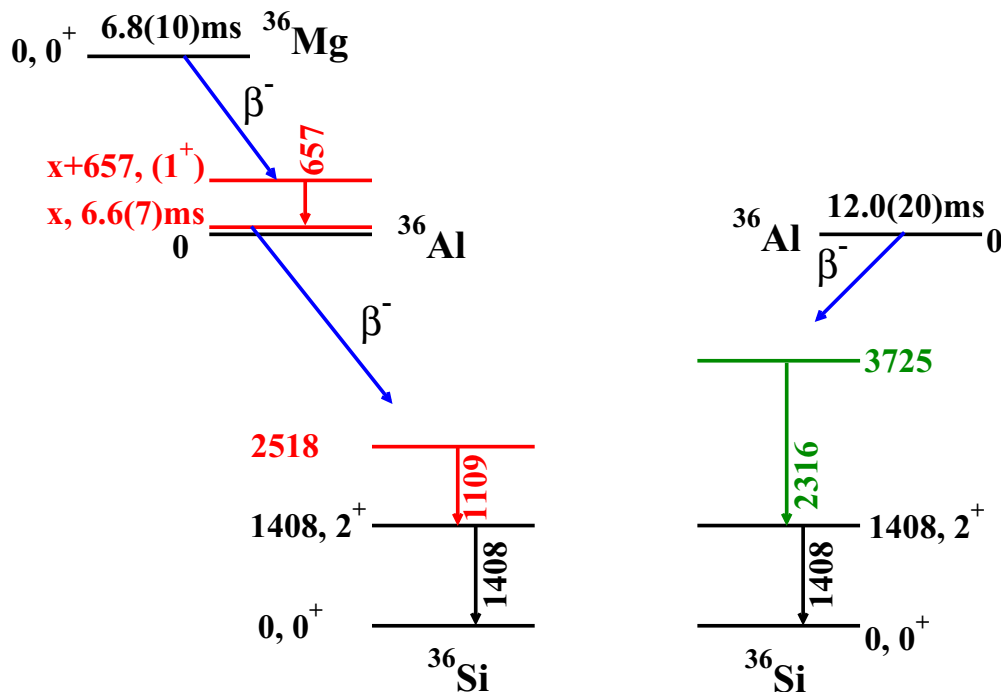


FIG. 3. Decay schemes of mass  $A = 36$  nuclei proposed from the current analysis. Only the  $\beta$ -0n branches are shown here. The levels and  $\gamma$ -ray transitions shown in red and green are newly assigned. We propose that the isomeric state of  $^{36}\text{Al}$  is favorably populated by the  $\beta$  decay of  $^{36}\text{Mg}$  (a similar procedure of the  $\beta$  decay of  $^{34}\text{Mg}$  [9,27]) and the ground state is strongly populated in the fragmentation reaction. However, the possibility of a vice-versa scenario cannot be excluded.

TABLE I. Observed excitation energies ( $E_x$ ), spin-parity ( $J^\pi$ ), together with the associated  $\beta$ -delayed  $\gamma$ -ray transitions ( $E_\gamma$ ) of  $^{36}\text{Si}$  deduced from the current experimental analysis from the decay of the isomeric and the ground state of  $^{36}\text{Al}$  are presented in this table. See the text for details.

Beam component $^{36}\text{Al}$	$E_x$ (keV)	$E_\gamma$ (keV)	$J_i^\pi$	$I_{\gamma,\text{rel}}$	$J_f^\pi$
Isomeric state	1408.4(2)	1408.4(2)	$2^+$	100	$0^+$
	2517.5(3)	1109.1(2)	$(2^+)$	46(5)	$2^+$
Ground state	1408.4(2)	1408.4(2)	$2^+$	100	$0^+$
	3724.7(3)	2316.3(2)	$(3^-)$	71(11)	$2^+$

1408 keV state, though the statistics prevented confirmation using  $\gamma$ - $\gamma$  coincidences. This assignment is made to  $^{36}\text{Si}$  because the neutron separation energy  $S_n$  of  $^{35}\text{Si}$  is only 2470 keV. Adding 2316 keV in cascade with the 910 keV level of  $^{35}\text{Si}$  places a level above  $S_n$ . A number of levels above  $S_n$  have been observed in  $^{35}\text{Si}$  following the  $\beta$  decay of  $^{35}\text{Al}$  as reported by Timis *et al.* [26], but there is no mention of a level at 3226 keV as would be required. The possibility of a ground-state transition cannot be excluded but there is no report of a level at 2316 keV in the literature [26], while a number of other ground-state transitions have been observed.

We will now focus on the two new transitions associated with  $^{36}\text{Si}$ , namely the 1109 keV and 2316 keV transitions. The transition at 1109 keV was observed in the  $\beta$  decay of  $^{36}\text{Mg}$  in both the NSCL and FRIB experiments, as shown in Fig. 1(a), 1(b). The peak is also seen, somewhat more weakly in the decay of  $^{36}\text{Al}$  in both data sets. Conversely, we have observed the 2316 keV peak in the  $\beta$  decay of  $^{36}\text{Al}$  in both data sets, but no sign in the decay of  $^{36}\text{Mg}$ . These observed discrepancies may suggest that the two states of  $^{36}\text{Si}$  decaying by the  $\gamma$ -ray transitions 1109 and 2316 keV are populated by different  $\beta$ -decay paths. This is possible if  $^{36}\text{Al}$  has a  $\beta$ -decaying isomer. This isomer can be favorably populated by the decay of  $^{36}\text{Mg}$  and  $\beta$  decays to the daughter nucleus  $^{36}\text{Si}$ . A very similar case has previously been observed in the  $\beta$  decay of  $^{34}\text{Mg}$  [9,27]. The decay scheme of the  $\beta$  decay of  $^{36}\text{Mg}$  and  $^{36}\text{Al}$  suggested from the current experimental observations is depicted in Fig. 3. It should be noted that the ordering of the isomeric and ground state in  $^{36}\text{Al}$  could be reversed. The level at 2518 keV in  $^{36}\text{Si}$  is populated in the  $\beta$  decay of proposed isomeric state of  $^{36}\text{Al}$  which is favorably populated in the decay of  $^{36}\text{Mg}$  into  $^{36}\text{Al}$ . The state at 3725 keV is populated by the  $\beta$  decay of the ground state of  $^{36}\text{Al}$ , which is the state primarily populated when  $^{36}\text{Al}$  is produced in the fragmentation reaction. The experimental observations also suggest that the isomer in  $^{36}\text{Al}$  was weakly present in the cocktail beam containing  $^{36}\text{Al}$  in both the experiments. Table I shows the energy states of  $^{36}\text{Si}$ , their spin-parity,  $\gamma$ -ray transitions, and the intensities relative to the 1408 keV transition deduced from the current analysis. To extract the relative intensities for the isomeric state, it was assumed that the  $\beta$  decay from  $^{36}\text{Mg}$  populated only the isomeric state in  $^{36}\text{Al}$  which subsequently decayed through the 1109 and 1408 keV transitions in  $^{36}\text{Si}$ . The directly produced  $^{36}\text{Al}$  was a mix of both isomeric and ground state and a small amount of the 1109 keV transition observed in Fig. 2 was attributed to the directly

produced  $^{36}\text{Al}$  isomeric state. The isomeric contribution was taken into account in deriving the presented relative intensities between the 1408- and 2316-keV transitions populated from the ground-state decay.

There is an additional transition at 1200 keV as seen in Figs. 1 and 2. At this time we do not have the statistics to perform  $\gamma$ - $\gamma$  coincidence analysis to place this transition, or determine the isotope with which it is associated, though it is most likely to be placed with  $^{35,36}\text{Si}$  based on its observation in both Figs. 1 and 2. The half-lives of  $^{36}\text{Mg}$  and  $^{36}\text{Al}$  have been reported before in Refs. [10,11,23,28]. Recently the half-life of  $^{36}\text{Mg}$  was measured from the same FRIB data set as 7.2(12) ms [19]. In the fit of Ref. [19] the daughter  $^{36}\text{Al}$  half-life was fixed at 90 ms based upon Ref. [10]. In the present work, we have additional information to disentangle and extract the half-lives of both  $^{36}\text{Mg}$  and  $^{36}\text{Al}$ . This analysis has been performed based upon the NSCL data. The half-life of the presumed  $^{36}\text{Al}$  ground state was extracted as 14.7(10) ms in the present work, as shown in the top panel of Fig. 4, which is close to that reported in Ref. [11] (see Fig. 1 of the Ref.) but far from the value quoted as 90(40) in Ref. [10]. The measured half-life of  $^{36}\text{Al}$  was further confirmed by fitting the decay time of events in coincidence with the 2316 keV peak of the daughter nucleus  $^{36}\text{Si}$  as seen Fig. 4(b). For the subsequent discussion, we have adopted a ground-state half-life of 12.0(20) ms for  $^{36}\text{Al}$ , based on the cleanest determination with the  $\gamma$ -ray gating.

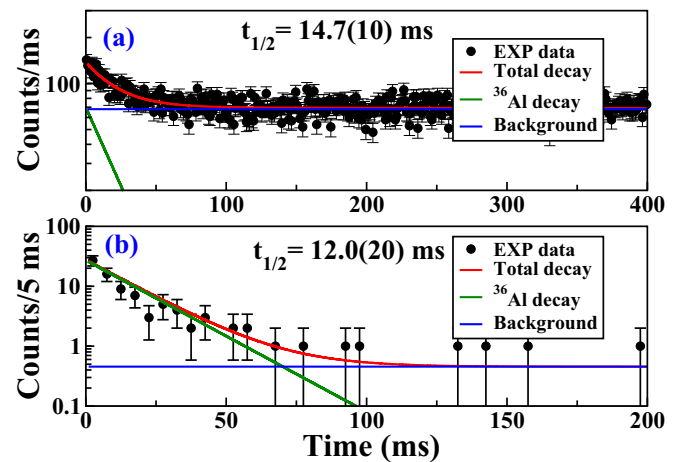


FIG. 4. (a)  $^{36}\text{Al}$  decay curve for a correlation time of 1500 ms between the implants and the  $\beta$  decay within 1 pixel. (b) Decay curve gated by the 2316 keV  $\gamma$ -ray transition from the  $\beta$ - $0n$  daughter  $^{36}\text{Si}$ .

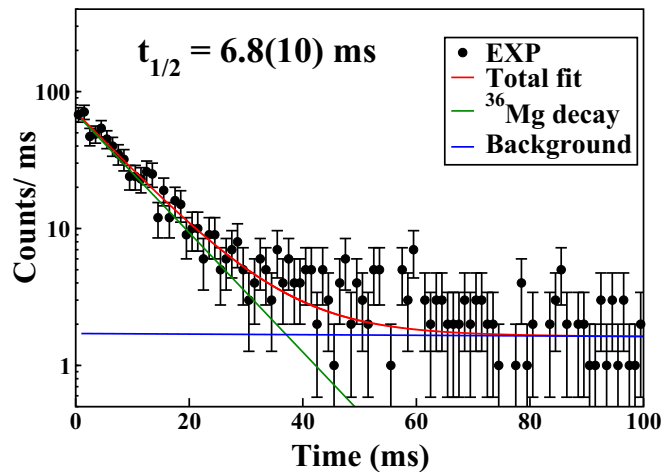


FIG. 5. Decay curve of  $^{36}\text{Mg}$  gated by the 657 keV  $\gamma$ -ray transition from the  $\beta$ -0n daughter  $^{36}\text{Al}$ .

In the case of  $^{36}\text{Mg}$ , the decay is hypothesized to feed the  $\beta$ -decaying isomer in  $^{36}\text{Al}$ , which introduces the uncertainty in fitting the total decay curve. As such, we focus for  $^{36}\text{Mg}$  on an exponential fit to the  $\gamma$ -ray transition gated time distribution of the 657 keV peak which gives a half-life of 6.8(10) ms as shown in Fig. 5.

The half-life of the isomeric state of  $^{36}\text{Al}$  has been measured by fitting the  $\gamma$ -peak gated time distributions of the 1109 keV and 1408 keV transitions, populated via  $\beta$  decay of  $^{36}\text{Mg}$ , with Batemann equations including the grow-in and decay of  $^{36}\text{Al}$ . The parent,  $^{36}\text{Mg}$ , half-life was kept fixed at 6.8 ms in the fits. The half-lives extracted for the  $^{36}\text{Al}$  isomeric state from the two fits were 6.6(11) and 6.5(10) ms, respectively, as shown in Fig. 6.

We do not have enough statistics with the FRIB data to measure the half-lives gated on the  $\gamma$ -ray transitions from the descendant nuclei. However, the  $^{36}\text{Mg}$  half-life extracted in

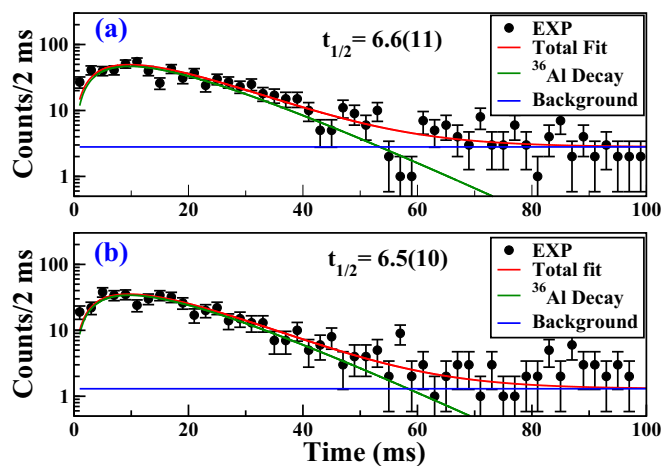


FIG. 6. Half-life of the suggested isomeric state of  $^{36}\text{Al}$  has been extracted from the  $\gamma$ -peak gated time distribution of the (a) 1408 keV and (b) 1109 keV transitions, populated via  $\beta$  decay of  $^{36}\text{Mg}$ .

this analysis is in good agreement within the error limits with that reported in Ref. [19].

#### IV. THEORETICAL DISCUSSION

The structure of  $^{36}\text{Al}$  has not been discussed before regarding the ground-state spin-parity or the observation of any  $\gamma$ -ray transitions. On the other hand, though  $^{36}\text{Si}$  has been studied in multiple experiments [10,29–32], no negative parity intruder states, which can be populated from  $\beta$  decay of  $^{36}\text{Al}$  via allowed  $\beta$  transitions, have been reported before. In this work, we report the observation of the excited states of  $^{36}\text{Al}$  and the possible negative-parity intruder state(s) of  $^{36}\text{Si}$  via  $\beta$ -delayed  $\gamma$ -ray spectroscopy.

The results from the current experimental analysis were compared with the shell model calculations performed with the FSU shell-model interaction [12,13] using the shell-model code CoSMo [33]. The FSU interaction covers a large part of the nuclear chart that includes nuclei ranging in mass number from around 10 to 50. It is a modern successor to a number of very successful effective interactions for individual shells supplemented with newly determined cross-shell matrix elements. In order to retain consistency, the effective interaction keeps the particle-hole hierarchy so that states of different harmonic oscillator excitation quanta  $\hbar\omega$  are not mixed.

The ground-state structure of  $^{36}\text{Al}$  is expected to be dominated by an odd number of neutrons in the  $fp$  shell and odd number of protons in the  $d_{5/2}$  orbital. This dominant configuration can provide a number of negative parity states closely spaced in energies. Shell-model calculations with the FSU interaction predict the ground state of  $^{36}\text{Al}$  as  $2^-$  for the  $0p0h (d_{5/2})^{-1} \otimes (f_{7/2})^3$  configuration. A degenerate  $4^-$  level is predicted at 7 keV as shown in Fig. 7. Among them, one can be the ground state and another can be the suggested isomeric state of  $^{36}\text{Al}$ . Considering the isomeric state is favorably populated by the  $\beta$  decay of  $^{36}\text{Mg}$ , a  $4^-$  ground state is more likely in which case the  $1^+$  state populated by the allowed  $\beta$  decay of  $^{36}\text{Mg}$  will decay to the  $2^-$  isomeric state by an  $E1$  transition which eventually will  $\beta$  decay to the excited state of  $^{36}\text{Si}$ . A  $\gamma$ -ray transition between the  $2^-$  and  $4^-$  levels would be hindered due to the very low energy gap with a  $B(E2)$  of 0.01 Wu according to the shell-model calculation. The lowest  $1p1h$  state in  $^{36}\text{Al}$  was predicted as  $1^+$  at 440 keV with respect to the predicted  $2^-$  level which can be the theoretical counterpart of the observed ( $1^+$ ) level that decays by the 657 keV transition to the proposed isomeric ( $2^-$ ) state.

With 14 protons and 22 neutrons, the ground-state configuration of  $^{36}\text{Si}$  will be dominated by the  $f_{7/2}$  neutrons with some occupancies in the  $1p_{3/2}$  orbital. Shell-model calculations with the FSU interaction have been performed for both  $0p0h$  and  $1p1h$  excitations in order to predict the positive and negative parity states, respectively. The calculated energy levels are compared with the observed states in the current experiments as well as those reported in the previous studies [34] and shown in Fig. 8.

The predicted positive parity levels are quite successful in reproducing the energies of the observed states of  $^{36}\text{Si}$ . The lowest-two positive parity levels  $0^+$  and  $2^+$  have significant contributions from the neutron  $1p_{3/2}$  orbital with occupancies

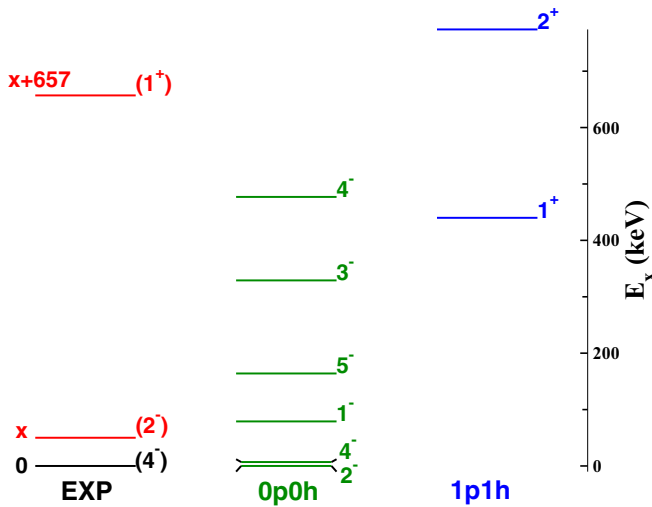


FIG. 7. Experimental energy states of  $^{36}\text{Al}$  observed in the present work are compared with those predicted by using the FSU shell-model interaction. We note that the relative ordering of the two  $\beta$ -decaying states could not be determined from the current analysis. Unmixed  $0\hbar\omega$  ( $0p0h$ ) and  $1\hbar\omega$  ( $1p1h$ ) states were calculated for the negative and positive parity levels, respectively, of  $^{36}\text{Al}$ . The levels in red have been newly observed in the current analysis and the spin-parity are suggested according to the shell-model predictions.

0.4 and 0.74, respectively. However, as the spin increases, the  $\nu 1p_{3/2}$  contribution decreases and the levels are more dominated by the  $\nu f_{7/2}$  occupancy. As the spin reaches to  $6^+$ , the state is of pure  $\nu(f_{7/2})^2$  configuration.

The shell-model predicts the first negative parity state of  $^{36}\text{Si}$  above 4 MeV as seen in Fig. 8. Considering a ( $4^-$ ) ground

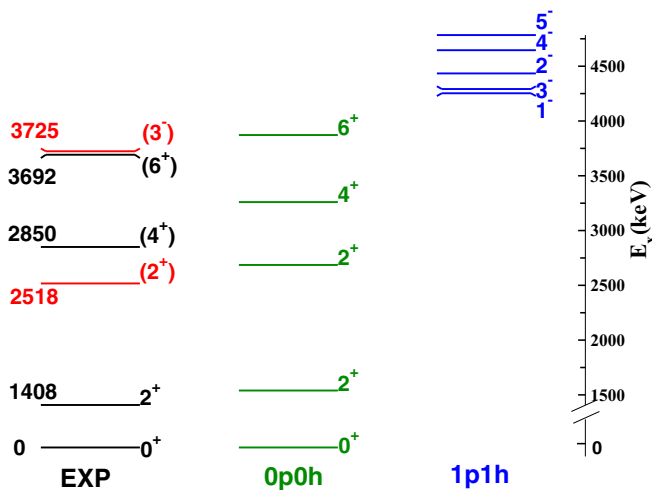


FIG. 8. Experimental energy states of  $^{36}\text{Si}$  observed in the present analysis as well as in the previous work [34] are compared with those predicted by using the FSU shell-model interaction. Unmixed  $0\hbar\omega$  ( $0p0h$ ) and  $1\hbar\omega$  ( $1p1h$ ) states were calculated for the positive and negative parity levels, respectively, of  $^{36}\text{Si}$ . The levels in red have been observed for the first time in the current analysis and the spin-parity are suggested according to the shell-model predictions.

state of  $^{36}\text{Al}$ , the observed level at 3725 keV of  $^{36}\text{Si}$  can be either of  $3^-$ ,  $4^-$ , or  $5^-$ . All of them have the same dominant configuration of  $(\nu d_{3/2})^{-1} \otimes (\nu f_{7/2})^3$  with  $1p_{3/2}$  occupancy  $\approx 0.5$ . The predicted  $3^-$  level at 4292 keV is a better energy match among them. A  $3^-$  spin-parity assignment to the 3725 keV level also follows the trend of the first negative parity state of the nearby even-mass Si isotopes [35–37]. The observed 2518 keV state does not have a suitable negative parity candidate in the current predictions. There is a good energy match with the second  $2^+$  state predicted at 2686 keV. If the 2518 keV level is of positive parity, this might have been populated either by a forbidden  $\beta$  transition or is fed by other negative parity levels at higher excitation energies whose  $\gamma$  rays were not observed in the current analysis.

## V. SUMMARY

The structure of  $^{36}\text{Al}$  has been studied for the first time with the observation of a  $\beta$ -decaying isomer. The  $\beta$ -decaying isomers in this region were previously reported in only two more nuclei, both are  $N > 21$  Al isotopes [27,32]. This is a unique structural property which deserves more investigation with the experimental data of enhanced statistics as well as with theoretical models capable of interpreting a wide range of isotopes in the same region.

In this work, the half-lives of  $^{36}\text{Mg}$  and  $^{36}\text{Al}$  have been measured. The half-life of  $^{36}\text{Mg}$  agreed well with the most recent measurements and that of  $^{36}\text{Al}$  was reported with a higher precision. An intruder opposite parity level of  $^{36}\text{Si}$  was populated and the lowest negative parity state was observed around 4 MeV. Shell-model predictions conducted by the FSU shell-model interaction quite successfully reproduce the experimental observations. The results of this study push forward our progress in understanding the structure of exotic nuclei. Evaluation of the level of configuration mixing will help refine theoretical interpretations in the future.

## ACKNOWLEDGMENTS

This work is supported partly by the US Department of Energy, Office of Science, Office of Nuclear Physics under Contracts No. DE-AC02-06CH11357 (ANL), DE-AC02-98CH10946 (BNL), DE-AC02-05CH11231 (LBNL), DE-AC52-07NA27344 (LLNL), DE-SC0020451 (Michigan State), DE-SC0014448 (Mississippi State), DE-AC05-00OR22725 (ORNL), DE-FG02-96ER40983 (UTK), and DE-FG02-94ER40848 (UML). The material was also sponsored by the US National Science Foundation under Grants No. PHY-2012522 (FSU), PHY-1848177 (CAREER) (Mississippi State), and PHY-1565546 (NSCL). The research was further sponsored by the US Department of Energy, National Nuclear Security Administration under Award No. DE-NA0003180 (Michigan State) and the Stewardship Science Academic Alliances program through DOE Awards No. DE-NA0003899 (UTK) and DOE-DE-NA0003906 (Michigan State), DE-SC0009883 (FSU) and NSF Major Research Instrumentation Program Award No. 1919735 (UTK). Discussions with B. A. Brown (FRIB, MSU) are gratefully acknowledged.

- [1] S. Michimasa, Y. Yanagisawa, K. Inafuku, N. Aoi, Z. Elekes, Z. Fülöp, Y. Ichikawa, N. Iwasa, K. Kurita, M. Kurokawa, T. Machida, T. Motobayashi, T. Nakamura, T. Nakabayashi, M. Notani, H. J. Ong, T. K. Onishi, H. Otsu, H. Sakurai, M. Shinohara *et al.*, *Phys. Rev. C* **89**, 054307 (2014).
- [2] H. L. Crawford, P. Fallon, A. O. Macchiavelli, A. Poves, V. M. Bader, D. Bazin, M. Bowry, C. M. Campbell, M. P. Carpenter, R. M. Clark, M. Cromaz, A. Gade, E. Ideguchi, H. Iwasaki, C. Langer, I. Y. Lee, C. Loelius, E. Lunderberg, C. Morse, A. L. Richard *et al.*, *Phys. Rev. C* **93**, 031303(R) (2016).
- [3] U. Datta, A. Rahaman, T. Aumann, S. Beceiro-Novo, K. Boretzky, C. Caesar, B. V. Carlson, W. N. Catford, S. Chakraborty, M. Chartier, D. Cortina-Gil, G. de Angelis, P. Diaz Fernandez, H. Emling, O. Ershova, L. M. Fraile, H. Geissel, D. Gonzalez-Diaz, B. Jonson, H. Johansson *et al.*, *Phys. Rev. C* **94**, 034304 (2016).
- [4] R. Elder, H. Iwasaki, J. Ash, D. Bazin, P. C. Bender, T. Braunroth, C. M. Campbell, H. L. Crawford, B. Elman, A. Gade, M. Grindler, N. Kobayashi, B. Longfellow, T. Mijatović, J. Pereira, A. Revel, D. Rhodes, and D. Weisshaar, *Phys. Rev. C* **104**, 024307 (2021).
- [5] H. Heylen, M. De Rydt, G. Neyens, M. L. Bissell, L. Caceres, R. Chevrie, J. M. Daugas, Y. Ichikawa, Y. Ishibashi, O. Kamalou, T. J. Mertzimekis, P. Morel, J. Papuga, A. Poves, M. M. Rajabali, C. Stödel, J. C. Thomas, H. Ueno, Y. Utsuno, N. Yoshida *et al.*, *Phys. Rev. C* **94**, 034312 (2016).
- [6] R. Han, X. Q. Li, W. G. Jiang, Z. H. Li, H. Hua, S. Q. Zhang, C. X. Yuan, D. X. Jiang, Y. L. Ye, J. Li, Z. H. Li, F. R. Xu, Q. B. Chen, J. Meng, J. S. Wang, C. Xu, Y. L. Sun, C. G. Wang, H. Y. Wu, C. Y. Niu *et al.*, *Phys. Lett. B* **772**, 529 (2017).
- [7] P. Himpe, G. Neyens, D. L. Balabanski, G. Bélier, D. Borremans, J. M. Daugas, F. de Oliveira Santos, M. De Rydt, K. Flanagan, G. Georgiev, M. Kowalska, S. Mallion, I. Matea, P. Morel, Y. E. Penionzhkevich, N. A. Smirnova, C. Stodel, K. Turzó, N. Vermeulen, and D. Yordanov, *Phys. Lett. B* **643**, 257 (2006).
- [8] P. Himpe, G. Neyens, D. L. Balabanski, G. Bélier, J. M. Daugas, F. de Oliveira Santos, M. De Rydt, K. T. Flanagan, I. Matea, P. Morel, Y. Penionzhkevich, L. Perrot, N. A. Smirnova, C. Stodel, J. C. Thomas, N. Vermeulen, D. T. Yordanov, Y. Utsuno, and T. Otsuka, *Phys. Lett. B* **658**, 203 (2008).
- [9] R. Lică, F. Rotaru, M. J. G. Borge, S. Grévy, F. Negoită, A. Poves, O. Sorlin, A. N. Andreyev, R. Borcea, C. Costache, H. De Witte, L. M. Fraile, P. T. Greenlees, M. Huyse, A. Ionescu, S. Kisiov, J. Konki, I. Lazarus, M. Madurga, N. Mărginean, N. Warr *et al.* (IDS Collaboration), *Phys. Rev. C* **95**, 021301(R) (2017).
- [10] P. L. Reeder, Y. Kim, W. K. Hensley, H. S. Miley, R. A. Warner, Z. Y. Zhou, D. J. Vieira, J. M. Wouters, and H. L. Seifert, *Proceedings of the International Conference on Exotic Nuclei and Atomic Masses, 19–23 June, Arles, France* (Springer, 1995), p. 587.
- [11] K. Yoneda, H. Sakurai, N. Aoi, N. Fukuda, T. Gomi, E. Ideguchi, N. Imai, H. Iwasaki, T. Kubo, Z. Liu *et al.*, *RIKEN Accel. Prog. Rep.* **594**, 78 (1998).
- [12] R. S. Lubna, K. Kravvaris, S. L. Tabor, V. Tripathi, A. Volya, E. Rubino, J. M. Allmond, B. Abromeit, L. T. Baby, and T. C. Hensley, *Phys. Rev. C* **100**, 034308 (2019).
- [13] R. S. Lubna, K. Kravvaris, S. L. Tabor, V. Tripathi, E. Rubino, and A. Volya, *Phys. Rev. Res.* **2**, 043342 (2020).
- [14] D. Morrissey, B. Sherrill, M. Steiner, A. Stolz, and I. Wiedenhoever, *Nucl. Instrum. Methods Phys. Res. B* **204**, 90 (2003), 14th International Conference on Electromagnetic Isotope Separators and Techniques Related to Their Applications.
- [15] W. Mueller, J. Church, T. Glasmacher, D. Gutknecht, G. Hackman, P. Hansen, Z. Hu, K. Miller, and P. Quirin, *Nucl. Instrum. Methods Phys. Res. A* **466**, 492 (2001).
- [16] M. Hausmann, A. Aaron, A. Amthor, M. Avilov, L. Bandura, R. Bennett, G. Bollen, T. Borden, T. Burgess, S. Chouhan, V. Graves, W. Mittig, D. Morrissey, F. Pellemoine, M. Portillo, R. Ronningen, M. Schein, B. Sherrill, and A. Zeller, *Nucl. Instrum. Methods Phys. Res. B* **317**, 349 (2013), XVIth International Conference on ElectroMagnetic Isotope Separators and Techniques Related to their Applications, December 2–7, 2012, Matsue, Japan.
- [17] FRIB decay station initiator proposal (2020), <https://fds.ornl.gov/wp-content/uploads/2020/09/FDSi-Proposal-May2020.pdf>.
- [18] FRIB decay station initiator (2022), <https://fds.ornl.gov/initiator/>.
- [19] H. L. Crawford, V. Tripathi, J. M. Allmond, B. P. Crider, R. Grzywacz, S. N. Liddick, A. Andalib, E. Argo, C. Benetti, S. Bhattacharya, C. M. Campbell, M. P. Carpenter, J. Chan, A. Chester, J. Christie, B. R. Clark, I. Cox, A. A. Doetsch, J. Dopfer, J. G. Duarte *et al.*, *Phys. Rev. Lett.* **129**, 212501 (2022).
- [20] R. Yokoyama, M. Singh, R. Grzywacz, A. Keeler, T. King, J. Agramunt, N. Brewer, S. Go, J. Heideman, J. Liu, S. Nishimura, P. Parkhurst, V. Phong, M. Rajabali, B. Rasco, K. Rykaczewski, D. Stracener, J. Tain, A. Tolosa-Delgado, K. Vaigneur *et al.*, *Nucl. Instrum. Methods Phys. Res. A* **937**, 93 (2019).
- [21] S. Paulauskas, M. Madurga, R. Grzywacz, D. Miller, S. Padgett, and H. Tan, *Nucl. Instrum. Methods Phys. Res. A* **737**, 22 (2014).
- [22] W. Peters, S. Ilyushkin, M. Madurga, C. Matei, S. Paulauskas, R. Grzywacz, D. Bardayan, C. Brune, J. Allen, J. Allen, Z. Bergstrom, J. Blackmon, N. Brewer, J. Cizewski, P. Copp, M. Howard, R. Ikeyama, R. Kozub, B. Manning, T. Massey *et al.*, *Nucl. Instrum. Methods Phys. Res. A* **836**, 122 (2016).
- [23] K. Steiger, PhD thesis, Technischen Universität München (2013).
- [24] B. V. Pritychenko, T. Glasmacher, B. A. Brown, P. D. Cottle, R. W. Ibbotson, K. W. Kemper, and H. Scheit, *Phys. Rev. C* **63**, 047308 (2001).
- [25] S. Chakraborty, U. Datta, T. Aumann, S. Beceiro-Novo, K. Boretzky, C. Caesar, B. V. Carlson, W. N. Catford, M. Chartier, D. Cortina-Gil, G. De Angelis, P. D. Fernandez, H. Emling, O. Ershova, L. M. Fraile, H. Geissel, D. Gonzalez-Diaz, H. Johansson, B. Jonson, N. Kalantar-Nayestanaki *et al.*, *Phys. Rev. C* **96**, 034301 (2017).
- [26] C. Timis, J. C. Angélique, A. Buta, N. L. Achouri, D. Baiborodin, P. Baumann, C. Borcea, S. Courtin, P. Dessagne, Z. Dlouhy, J. M. Daugas, S. Grévy, D. Guillemaud-Mueller, A. Knipper, F. R. Lecolley, J. L. Lecouey, M. Lewitowicz, E. Liénard, S. M. Lukyanov, F. M. Marqués *et al.*, *J. Phys. G: Nucl. Part. Phys.* **31**, S1965 (2005).
- [27] R. Lică, F. Rotaru, M. J. G. Borge, S. Grévy, F. Negoită, A. Poves, O. Sorlin, A. N. Andreyev, R. Borcea, C. Costache, H. De Witte, L. M. Fraile, P. T. Greenlees, M. Huyse, A. Ionescu, S. Kisiov, J. Konki, I. Lazarus, M. Madurga, N. Mărginean, C. A. Ur *et al.* (IDS Collaboration), *Phys. Rev. C* **100**, 034306 (2019).

- [28] S. Grévy, J. Angélique, P. Baumann, C. Borcea, A. Buta, G. Canchel, W. N. Catford, S. Courtin, J. Daugas, F. de Oliveira, P. Dessagne, Z. Dlouhy, A. Knipper, K. L. Kratz, F. Lecolley, J. Lecouey, G. Lehrseneau, M. Lewitowicz, E. Liénard, S. Lukyanov *et al.*, *Phys. Lett. B* **594**, 252 (2004).
- [29] C. Campbell, N. Aoi, D. Bazin, M. D. Bowen, B. A. Brown, J. M. Cook, D.-C. Dinca, A. Gade, T. Glasmacher, M. Horoi, S. Kanno, T. Motobayashi, L. A. Riley, H. Sagawa, H. Sakurai, K. Starosta, H. Suzuki, S. Takeuchi, J. R. Terry, K. Yoneda *et al.*, *Phys. Lett. B* **652**, 169 (2007).
- [30] X. Liang, F. Azaiez, R. Chapman, F. Haas, D. Bazzacco, S. Beghini, B. R. Behera, L. Berti, M. Burns, E. Caurier, L. Corradi, D. Curien, A. Deacon, G. d. Angelis, Z. Dombradi, E. Farnea, E. Fioretto, A. Hodsdon, A. Gadea, F. Ibrahim *et al.*, *Phys. Rev. C* **74**, 014311 (2006).
- [31] R. W. Ibbotson, T. Glasmacher, B. A. Brown, L. Chen, M. J. Chromik, P. D. Cottle, M. Fauerbach, K. W. Kemper, D. J. Morrissey, H. Scheit, and M. Thoennessen, *Phys. Rev. Lett.* **80**, 2081 (1998).
- [32] K. Steiger, S. Nishimura, Z. Li, R. Gernhäuser, Y. Utsuno, R. Chen, T. Faestermann, C. Hinke, R. Krücken, M. Kurata-Nishimura, G. Lorusso, Y. Miyashita, N. Shimizu, K. Sugimoto, T. Sumikama, H. Watanabe, and K. Yoshinaga, *Eur. Phys. J. A* **51**, 117 (2015).
- [33] A. Volya, Continuum Shell Model code, <https://www.volya.net/>.
- [34] N. Nica, J. Cameron, and B. Singh, *Nucl. Data Sheets* **113**, 1 (2012).
- [35] M. Shamsuzzoha Basunia, *Nucl. Data Sheets* **111**, 2331 (2010).
- [36] C. Ouellet and B. Singh, *Nucl. Data Sheets* **112**, 2199 (2011).
- [37] N. Nica and B. Singh, *Nucl. Data Sheets* **113**, 1563 (2012).